Textures and Microstructures, 1995, Vol. 24, pp. 75–91
Reprints available directly from the publisher
Photocopying permitted by license only

TEXTURE AND MICROSTRUCTURE IN HOT-PRESSED Si_3N_4

T. WALKER*, N. MATTERN* and M. HERRMANN**

**Institut für Festkörper- und Werkstofforschung Dresden e.V.*
***Fraunhofer Institut für Keramische Technologien und Sinterwerkstoffe, Dresden*

(Received 10 September 1994; in final form 7 November 1994)

The texture formation in hot-pressed Si_3N_4-ceramics was investigated by means of X-ray diffraction. A ring-fibre texture is observed with the basal plane (002) perpendicular to the hot-pressing axis. The texture index of hot-pressed Si_3N_4 depends on the starting powder mixture and process parameters. The $\alpha \rightarrow \beta$ phase transfomation and the growth of β-Si_3N_4 needlelike grains are correlated with the texture. Measurements of fracture toughness and aspect ratio confirm the correlation with microstructure. The structure is the result of crystal growth and flow process during hot-pressing.

KEY WORDS: Ceramic-materials, Si_3N_4, hot-pressing, texture, microstructure.

1. INTRODUCTION

Due to their high abrasion strength (deterioration) and good mechanical properties (Aldinger *et al.*, 1992) Si_3N_4 materials are promising for their application as engine and machine components and for purposes of wear resistance.

Strengthening mechanisms as crack-deflection, crack-bridging and crack-branch lead to a high strength and fracture toughness.

These mechanisms will be created by the formation of needlelike β-Si_3N_4-grains during sintering.

The main phase of the Si_3N_4-initial powder is the metastable α-Si_3N_4-modification. The transformation into the stable β-modification occurs during compaction by solution-diffusion-precipitation mechanisms. The β-Si_3N_4-grains grow anisotropically and from needles with a hexagonal cross-section.

A nearly isotropic orientation of the β-needles will form during sintering of green bodies by the globular shape of the initial powder. In contrast, hot-pressing due to the axially effective pressure during compression leads to macroscopic flow (Keßler *et al.*, 1991). The needles will be arranged perpendicularly to the hot-pressing direction. The result is an anisotropy of the mechanical properties (Lee *et al.*, 1992).

In this paper, the influence of the production conditions such as sintering aid, isothermal time and the load-application point on the texture will be investigated. The correlation of the X-ray measured and analysed orientation distributions with microstructure will be shown. An idea of texture formation will be derived from experimental investigations.

Table 1 Characteristics of the used powders.

Powder	*Producer*	*Oxygen content* %	*Specific surface* m^2/g	*Grain size* μm	$\alpha/(\alpha + \beta)$ %
SNE-10	INCH, Riga	1.6	11.9	0.54	97.3
LC12SX	HCST	2.1	17.8	0.69	97.6
PP1	UBE, Ind.	2.1	19.0	0.50	48.4

2. EXPERIMENTAL PROCEDURE

2.1 *Si_3N_4-Starting Powder*

Different starting powders of Si_3N_4 were used and are listed in Table 1. Preliminary investigations (Pabst *et al.*, 1993) have shown that powders of a specific surface and phase composition originate from different production technologies, differences in densification behaviour and in phase transformation.

2.2 *Preparation Technology*

Sintering additives (yttrium-aluminium-garnet) composed by the weight ratio of Y_2O_3 to Al_2O_3 of 5:1 were added to the Si_3N_4-powders. The additive was mixed with Si_3N_4 in isopropanol. The subsequent treatment consists of grinding in an attritor for 4 hours. After drying a sieve granulation was carried out. It follows a calcination of the blend.

An exemplary hot-pressing regime is shown in Figure 1. The samples are heated up to 1500°C. At this temperature the load is applied slowly to the hot-pressing process.

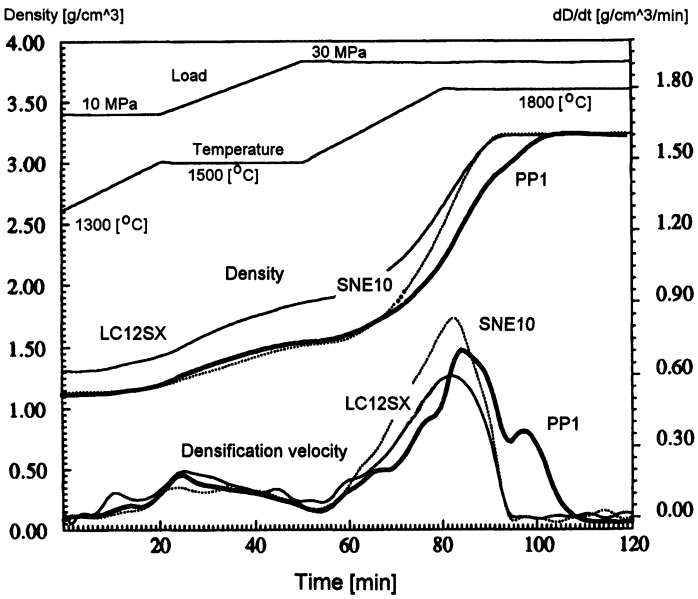

Figure 1 Densification curve of the powders LC12SX (890), SNE-10 (878) and PP1 (914) [Additive content: 5 Y_2O_3 + 1 Al_2O_3].

Table 2 Summary of hot-pressing conditions (Y: Y_2O_3; Al: Al_2O_3).

Parameter:	*Different conditions:*
Powder	SNE-10; LC12SX; PP1
Additive [%]	3Y + 0.6Al; 4Y + 0.8Al; 5Y + 1A1; 10Y + 2A1
Isothermal time 1800°C in [min]	0; 30; 60; 90
Moment of the load [°C]	1500; 1700; 1750

Afterwards the temperature is increased up to 1800°C over 30 minutes. It follows a 60 minutes isothermal time.

The different hot-pressing conditions are given in Table 2. Next to several powders the additive quantity, the temperature of the load-application and the isothermal cycles were varied.

From different stages of the process samples were taken. The samples (10 mm *10 mm *6 mm) were taken from the hot-pressing-plate. The top surface of all samples were removed by grinding.

2.3 *X-ray Analysis*

For the texture analysis of the α- and β-Si_3N_4 phase incomplete pole figures according to Table 3 were measured. The sample surface was perpendicular to the hot-pressed direction. The measurement were carried out with a texture goniometer in reflection geometry using Co Kα radiation. The range for the tilt angle ψ was chosen between 0° and 75° and for the rotation angle φ between 0° in 355° in 5° intervals.

From the measurement of several pole figures with independent **hkl** the three-dimensional orientation distribution function (ODF) was calculated using the series expansion method (Bunge, 1969). The ODF describes the volume fraction of crystallites with a specific orientation **g** with respect to a sample reference system.

The ODF allows the calculation of unmeasurable pole figures. In our case the basal pole figure *(001)* of the β-Si_3N_4 can be used to obtain an impression of the preferred orientation of the c-axis.

Pole densities are expressed in multiples of the random density (mrd-units).

2.4 *Microstructure Investigations*

In contrast to isotropic materials the investigations of anisotropic materials require at least two cuts in two different directions. For hot-pressing ceramics the greatest differences are assumed parallel and perpendicularly to the hot-pressing direction.

Table 3 The measured (hkl)-peaks.

α-Si_3N_4			β-Si_3N_4		
hkl	*Intensity*	*d-Value*	*hkl*	*Intensity*	*d-Value*
101	78	4.309	200	100	3.293
201	100	2.882	101	99	2.660
210	99	2.538	210	93	2.489
301	44	2.079	301	37	1.752

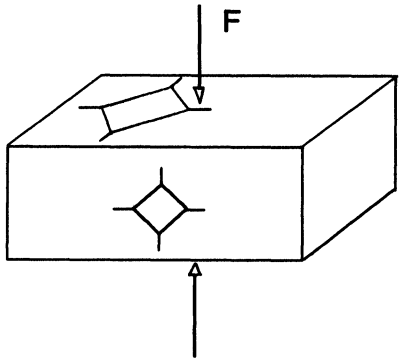

Figure 2 Position of Vickers indenter in the samples. F: hot-pressing direction.

Therefore the cuts were prepared in these planes. For the microstructural analysis the samples were prepared by plasma etching with CF_4. Afterwards the samples were covered with a layer of gold to produce a conductive surface for the scanning electron microscopy (SEM). An image processing system took the photos for the semi-automatic aspect ratio measurements.

2.5 *Toughness Measurements*

Indentation fracture toughness measurements were performed using Vickers indentation at 10 kg. The determination of toughness anisotropy requires a Vickers indenter parallel and perpendicularly to the sample normal direction (Figure 2). One axis was aligned to the pressing direction. The fracture lengths could be measured under a microscope. For the calculation the formula according to Anstis (Munz *et al.*, 1989) was used.

3. RESULTS AND DISCUSSION

3.1 *Phase Transformation*

Figure 3 shows an exemplary X-ray diffraction pattern of the powder SNE-10 after several hot-pressing states. The reflections depict the phase transformation from α- to β-Si_3N_4. The quantitative phase analysis (Table 4) describes the transformed quantity during the process (Mattern *et al.*, 1993). After isothermal annealing for 90 min only the β-Si_3N_4 phase is observed.

The phase transformation starts with the occurrence of the liquid phase at approximately 1400°C. The sintering process requires a liquid phase for the dissolution-reprecipitation of the Si_3N_4 due to small self-diffusion. Transformation of the crystalline Si_3N_4 of the α-modification into β-grains takes place during the sintering process. The liquid phase forms by the reaction of the sintering additives and SiO_2 at the surface of Si_3N_4

The occurrence of the two maxima in the densification rate (Figure 1) represents on the one hand the reduction of pores due to the rearrangement and viscous flow processes during the densification and on the other hand the dissolution-reprecipitation process (Keßler, 1993).

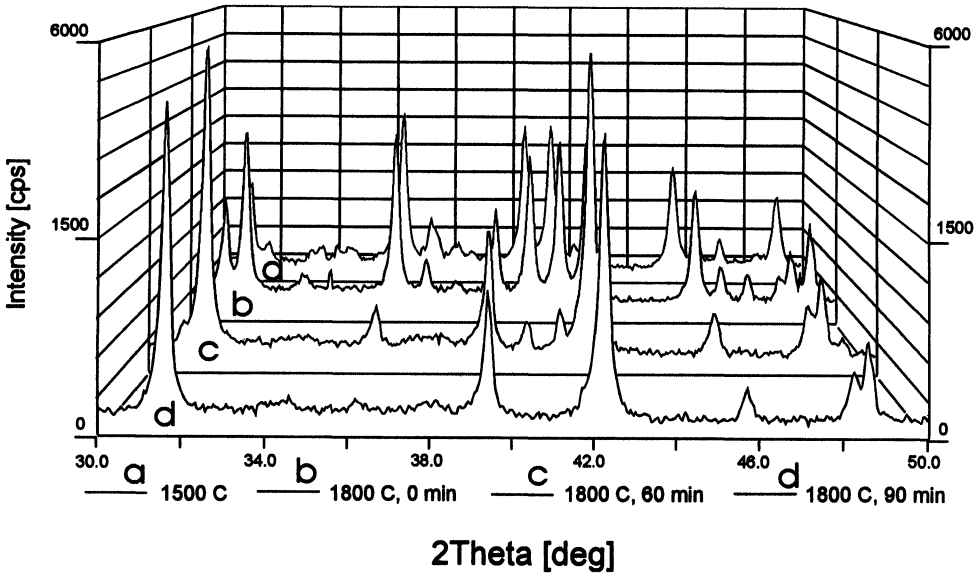

Figure 3 The α-β phase development of Si_3N_4 during the hot-pressing process.

Table 4 The α and β-phase quantity at different stages of the hot pressing process for the powder SNE 10 with 5 Y_2O_3 and 1 Al_2O_3.

			Isothermal Time [min] at 1800°C			
	Initial Part	*At 1500°C*	*0*	*30*	*60*	*90*
α-Phase [wt%]	97.0	97.0	64.4	15.0	4.9	0
β-Phase [wt%]	3.0	3.0	35.6	85.0	95.1	100.0
Density [g/cm^3]	–	1.533	2.970	3.233	3.246	3.252

A large amount of the densification occurs between 1500 and 1800°C (Figure 1). In contrast, the α-β transformation with the growth of the β-grains continues to take place during isothermal annealing at 1800°C.

3.2 *Texture Formation*

The texture analysis of the α- and β-Si_3N_4 phase was carried out with the **hkl**, presented in Table 3.

The measured pole figures of the α-phase show in all cases the absence of preferred orientation. The texture index J defined as an integral over the texture function f(g) ($J = \oint[f(g)]^2 dg$) is nearly 1 (random) for the α-Si_3N_4-phase (Bunge, 1987).

In contrast to the α-phase the β-Si_3N_4-phase (Figure 4) shows a ring-fibre texture (Wassermann *et al*,. 1962). All planes perpendicular to the basal plane (002) show the maximum in the center of the pole figure, e.g. (200), (210). The maxima of the pole figures (101) and (301) are situated on a circle. The circles are tilted to an angle of

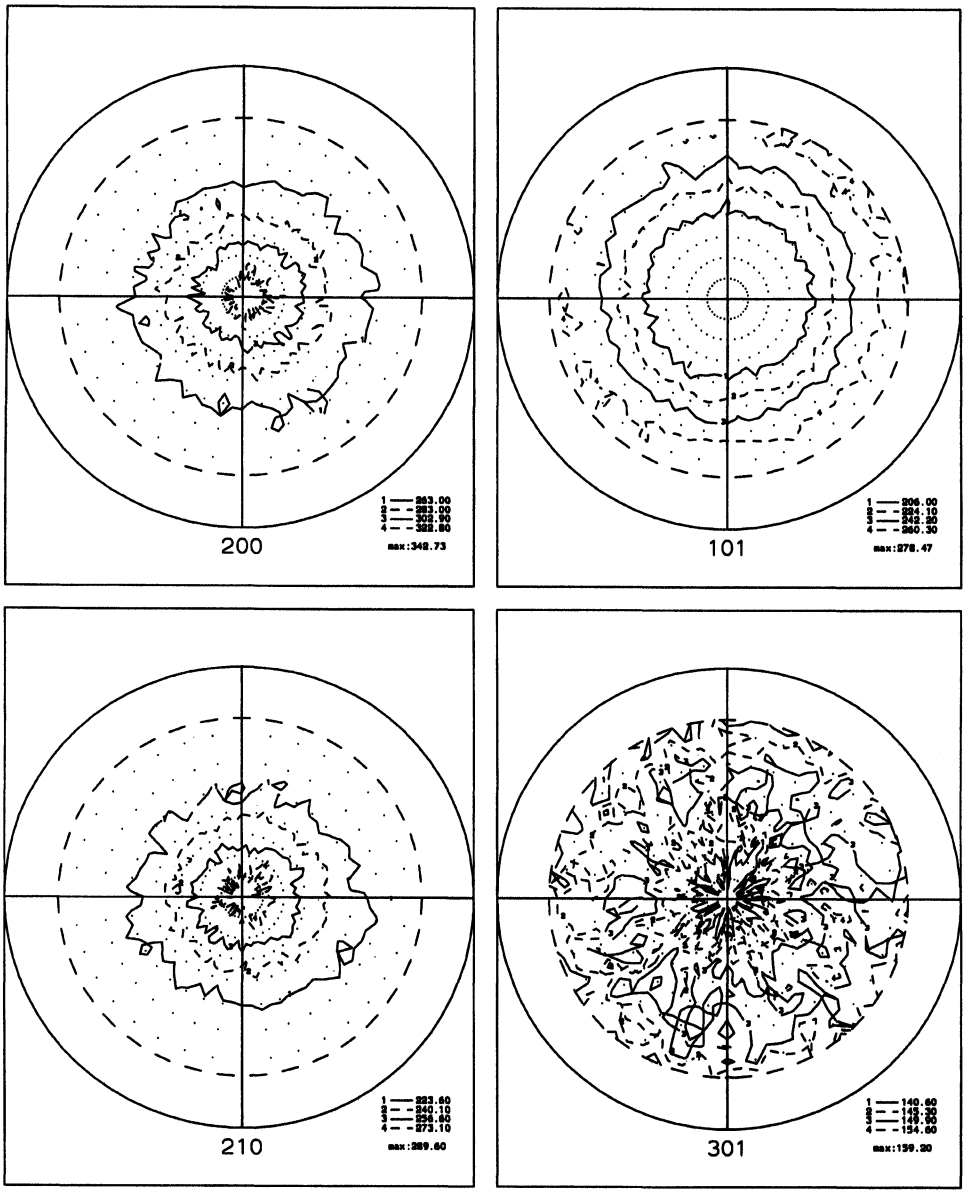

Figure 4 The measured pole figures (200), (101), (210) and (301) of the β-phase of a hot-pressed Si_3N_4 sample.

66.2° and 37.0° to the center of the pole figure, respectively. Accordingly the texture is arranged rotational-symmetrical to the sample normal. The FWHM (Full Width Half Maximum) of the measured peaks are relatively great. The values are between 90° and 120°.

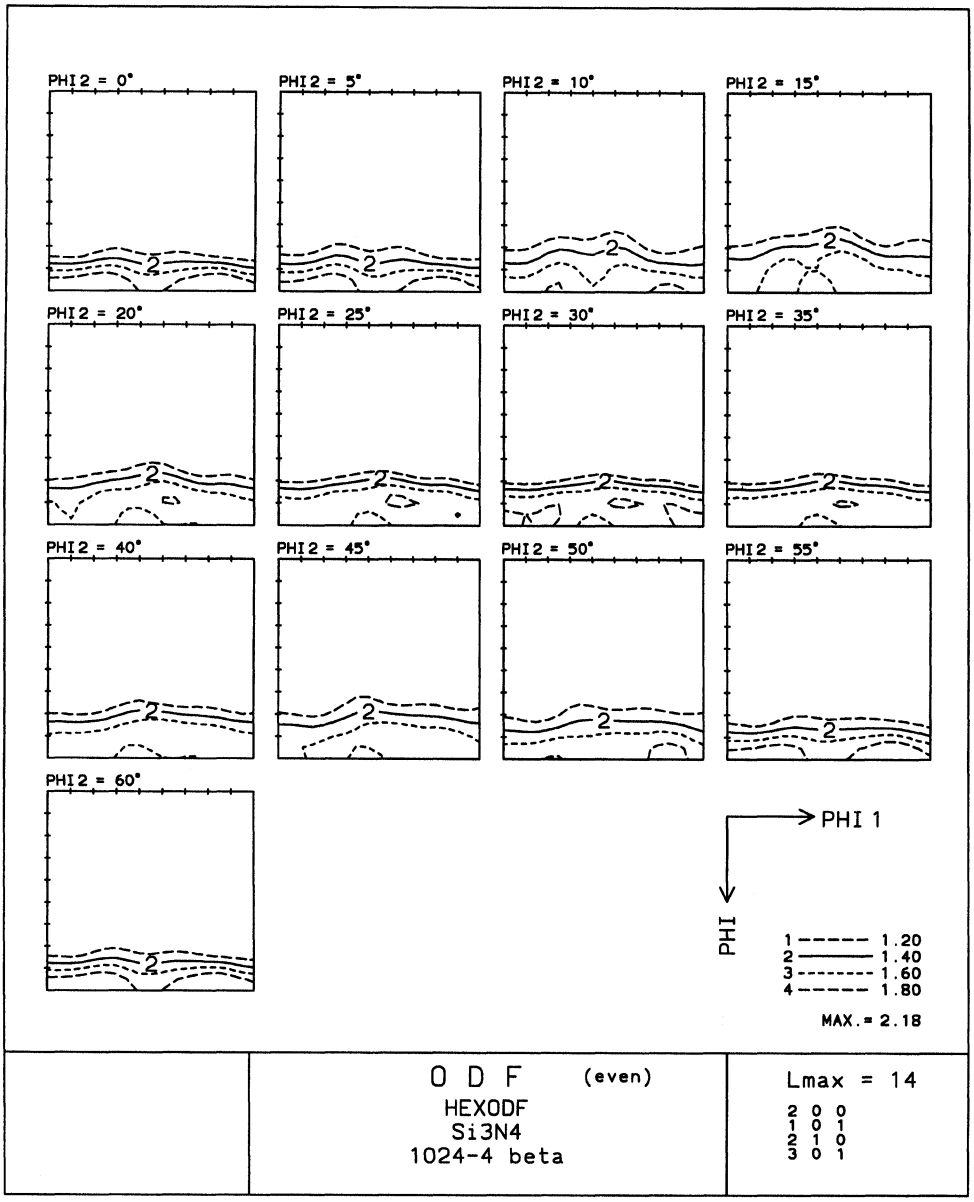

Figure 5 The orientation distribution function of the β-phase of a hot-pressed Si_3N_4 sample.

The Orientation Distribution Function (Figure 5) confirmed the rotational-symmetry. The maxima are situated on a line with $\phi = 90°$ and $\varphi_2 = 0°$ in the Euler space. The position of the line is nearly independent of the angle φ_1. The location corresponds to an orientation of the (002) basal plane perpendicular to the hot-pressing direction.

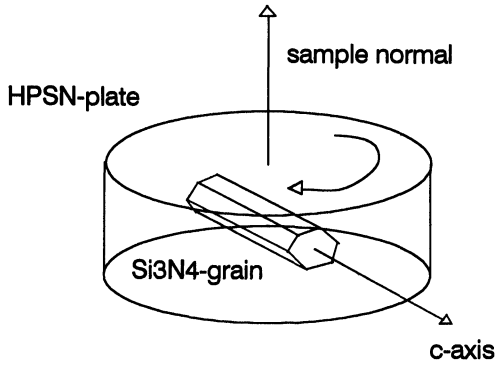

Figure 6 A simplified representation of the arrangement of the Si_3N_4-grains.

A simplified representation of the orientation of the Si_3N_4-grains is drawn in Figure 6. The dispersion of the needles amounts to 30 ±5° about the c-axis.

3.3 *Influence of Preparation Conditions on the Texture Index*

3.3.1 *Powder Characteristics*

Figure 1, presents the differences in the densification behaviour of the powders used. The powder SNE-10, the production of which is based on the Diimid-synthesis, densificates slower than the powder LC12SX which was produced through the nitration of silicon. The result is a higher texture index (Figure 7). The powder PP1 that was plasma-chemically manufactured shows the slowest densification. The texture index

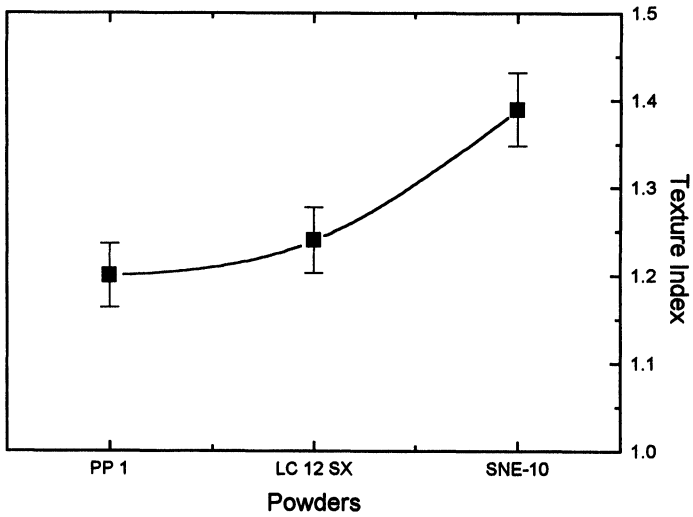

Figure 7 The correlation between the texture index and different starting powders for the same process regime.

remains low because 50% of the originate powder was already in the β-phase. Therefore only half of the powder takes part in the α-β-transformation. This leads to reduced anisotropy.

Other reasons for the differences in the densification behaviour can be found in the varying specific surfaces, the different grain sizes and oxygen contents (Table 1).

3.3.2 *Sintering Aid*

Sintering aids support the flow process during hot-pressing. A definite quantity of sintering aid is required for a total densification, dependent on powder characteristics (granulometric state, phase composition, oxygen and impurity content). An increased additive content reduces the time of densification but a lower additive content yields a better high-temperature strength (Schubert *et al.*, 1989).

The increase of additives leads to an acceleration of the densification process. This can be attributed to accelerated rearrangement processes and macroscopic flow processes.

The phase transformation rate remains nearly unchanged.

Therefore the densification by rearrangement and viscous flow is finished, when only a small part of β-Si_3N_4-needles exist and the orientation of the grains is not so pronounced.

To achieve a high texture it is necessary to use a minimum of sintering aid. Figure 8 shows that the texture index decreases with increasing content of additives. A disadvantage, on the other hand, is that the danger of locally inhomogeneous density rises due to insufficient viscosity.

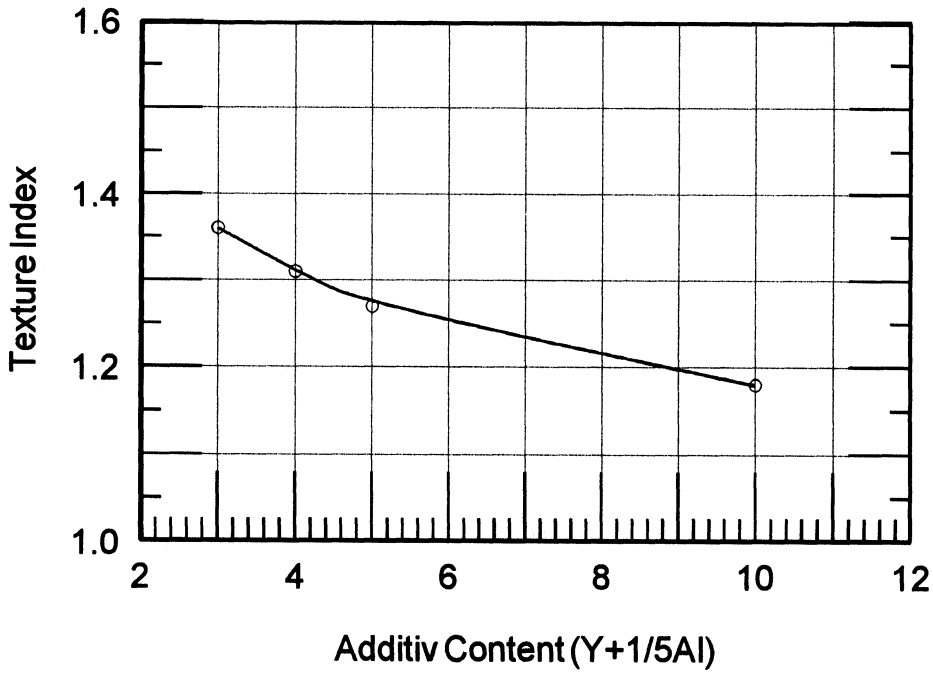

Figure 8 Dependence of the texture index on the additive content.

The result gives evidence, that for texture forming rearrangement- and grain-rotation-processes, respectively, play an important role.

3.3.3 *Isothermal Time*

After reaching the hot-pressing temperature, the temperature remained constant for a definite time. During this isothermal time the most part of the α-β-transformation takes place. With the enlargement of the β-Si_3N_4-phase fraction the preferred orientation increases. In Figure 9 the evolution of the β-phase content in wt% and the texture index for several isothermal times are given.

The duration of isothermal time at 1800° slightly reinforces texture strength of β-Si_3N_4. The reason for the increase of the preferred orientation is found in the preferred nucleation and grain growth contributing to preferred orientation. Whereas the additive content influences the texture strength by the grain rotation mechanism, the length of the isothermal cycles leads to an additional reinforcement of the texture by the texture formation mechanism. Results given by Lee and Bowman (Lee *et al.*, 1992) demonstrate the texture strengthening effect.

3.3.4 *Load-application Point*

During hot-pressing, the compaction behaviour of Si_3N_4 can be influenced by the temperature of the load-application point (pressurization). The load is applied to the samples at 1700° and 1750°, respectively. Despite the higher temperature at the moment of loading, the samples present a retarded compaction in the isothermal range. Table 5 lists the corresponding texture data.

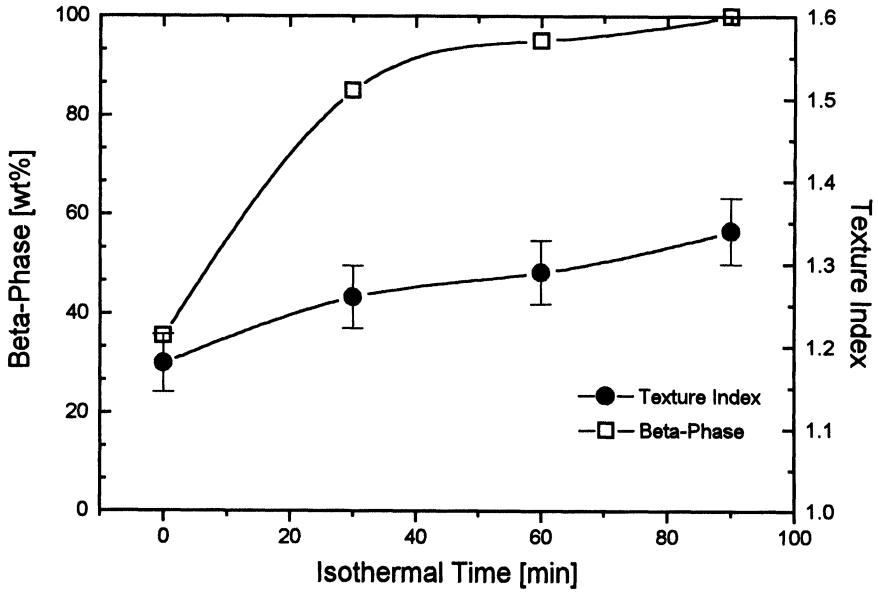

Figure 9 The development of the texture index and the β-phase quantity dependence on the isothermal time of the powder SNE10.

Table 5 The texture index dependence on the load-application.

Si_3N_4 Powder SNE 10			
Sample	878	903	1029
Temperature of load-application [°C]	1500	1700	1750
Texture Index	1.27	1.41	1.44

The mechanism of the texture reinforcement is discussed by Schubert and Pabst (Schubert *et al.*, 1989). The cause of the impeded compaction is attributed to the presence of β,β'-transcrystals that develop below 1700°C. The β,β'-transcrystals form a relatively rigid framework at the particle-points of contact. The result is a steric hindrance to the processes of rearrangement and flow.

Whereas the delayed compaction yields a reinforcement of the texture strength, the microscopic homogenization of the microstructure will be impaired. The result is a lowering of the materials K_c-value and the strength.

3.4 *Correlation between Microstructure and Texture*

3.4.1 *Microstructure*

Figures 10–12 show SEM-micrographs of Si_3N_4 powders of different origin. All samples were heated up to 1800° and had an isothermal time of 60 min. The micrographs were taken perpendicularly to the hot-pressing direction.

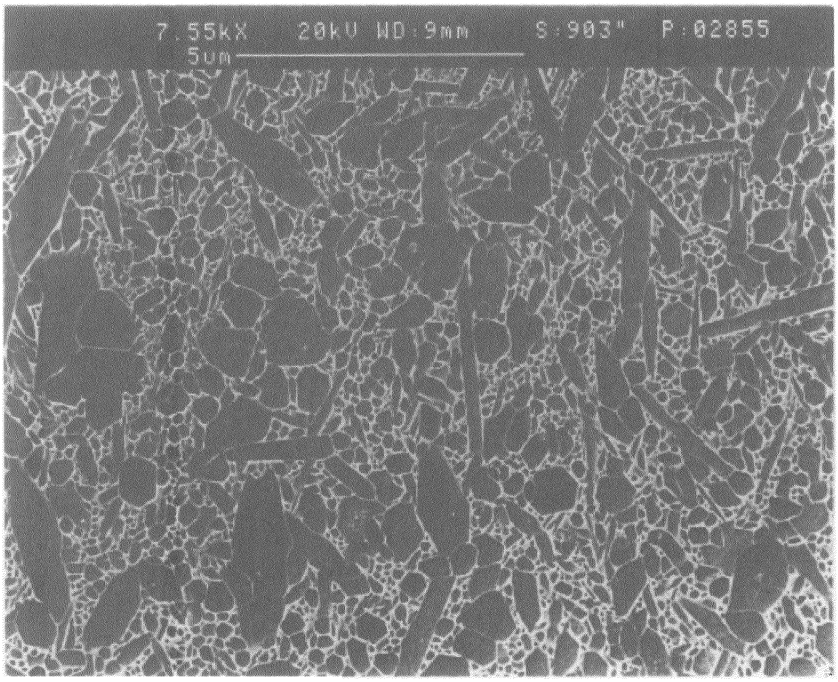

Figure 10 The microstructure of hot-pressed Si_3N_4 of the sintering powder SNE-10 perpendicular to the hot-pressing direction.

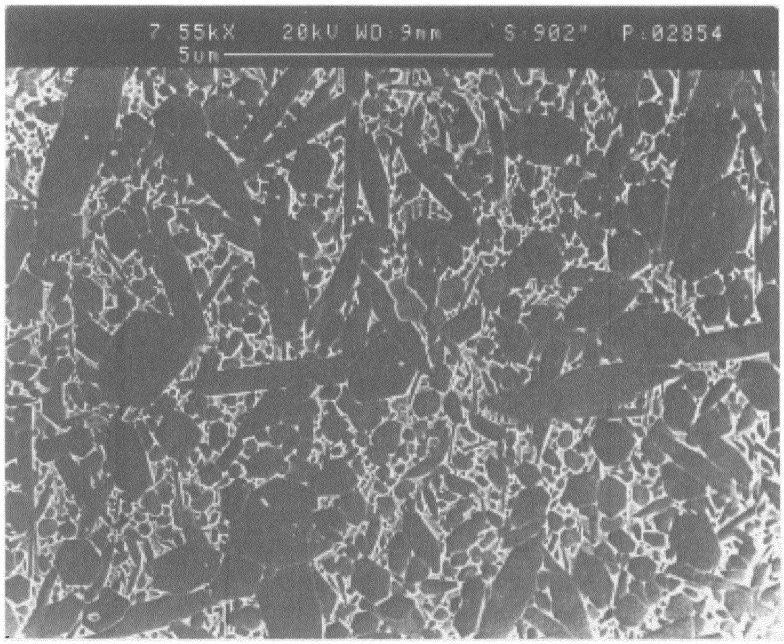

Figure 11 The microstructure of hot-pressed Si_3N_4 of the sintering powder LC12-SX perpendicular to the hot-pressing direction.

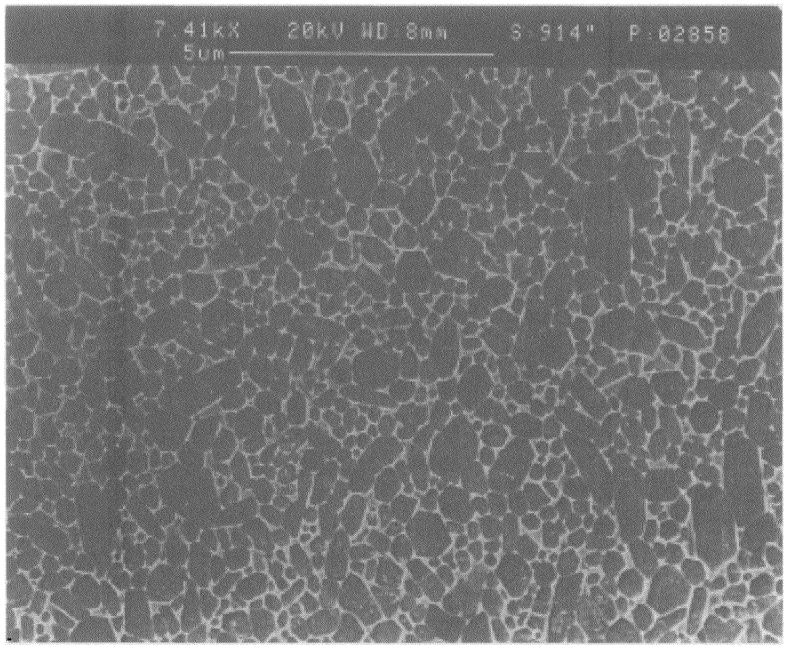

Figure 12 The microstructure of hot-pressed Si_3N_4 of the sintering powder PP1 perpendicular to the hot-pressing direction.

The dark areas are the β-phase of the Si_3N_4. The β-grains are surrounded by the amorphous grain-boundary phase, which appears as a bright matrix. The micrographs show both rounded and needle like crystallites of the β-phase. The needle axis is the [001]-direction or c-axis. The result corresponds to the X-ray measurements. All figures present a few large and a lot of small grains. The grain growth happens preferably on large grains, which define the texture.

The plasma-chemically manufactured powder (Figure 12) shows in comparison with the other samples a considerably more homogeneous microstructure. Already at the beginning 50% of the material is in the β-phase. As a consequence a smaller part of the β-phase is formed with a preferred orientation during hot-pressing. The result is a weaker texture. Correspondingly the aspect ratio of length to thickness of the grains is smaller. That is why there is no smaller driving force for rotation of the grains in the plane

3.4.2 *Aspect Ratio*

For the characterization of microstructure a method can be applied, which allows the determination of the real aspect ratio of β-Si_3N_4 grains (Herrmann *et al.*, 1992). The analysis starts with polished and etched sections of the Si_3N_4 material.

To describes microstructures a form factor was introduced as the ratio between length and thickness of needle-like grains. This aspect ratio cannot be determined directly from a polished section because only a small part of the grains will be cut in the correct plane. To obtain the real volume aspect ratio it is necessary to convert the measured, apparent aspect ratio distribution to the real one.

The method for isotropic Si_3N_4 microstructure is based on the assumption, that all grains have the shape of prisms with a hexagonal basal plane. The assumption is not completely fulfilled but other assumptions supply a greater error (Herrmann *et al.*, 1992).

The conversion of the apparent aspect ratio into the real one is based on the following steps:

- the probability of grain cuts in dependence on the angle ϕ between the needle axes and the cut-plane has to be calculated for all angles;
- the aspect ratio has to be determined for the created polished sections.

The result is a distribution curve for the apparent aspect ratio.

In isotropic microstructures the distribution of needles can be described in dependence on the angle ϕ to the cut-plane by a circle section:

$$dP(\phi) = C * \cos\phi \, d\phi \tag{1}$$

with C as the normalization factor. In contrast, in hot-pressing uniaxial, anisotropic materials the probability is proportional to the section of a rotational-ellipsoid with two equal main axes perpendicular to hot-pressing direction. The main axis in pressing direction is lower. Therefore the probability varies for different directions. The squares of the main axes are proportional to the number of oriented needles in this direction.

Therefore the ratio of the main axes can be compared with X-ray measured anisotropy. The ratio of the intensities of (002)-peaks perpendicular and parallel to the hot-pressing direction is called the anisotropy factor.

The relationship between the anisotropy-factor and the ratio of grain parts with an apparent aspect ratio > 3.5 of the total number of grains is theoretically calculated.

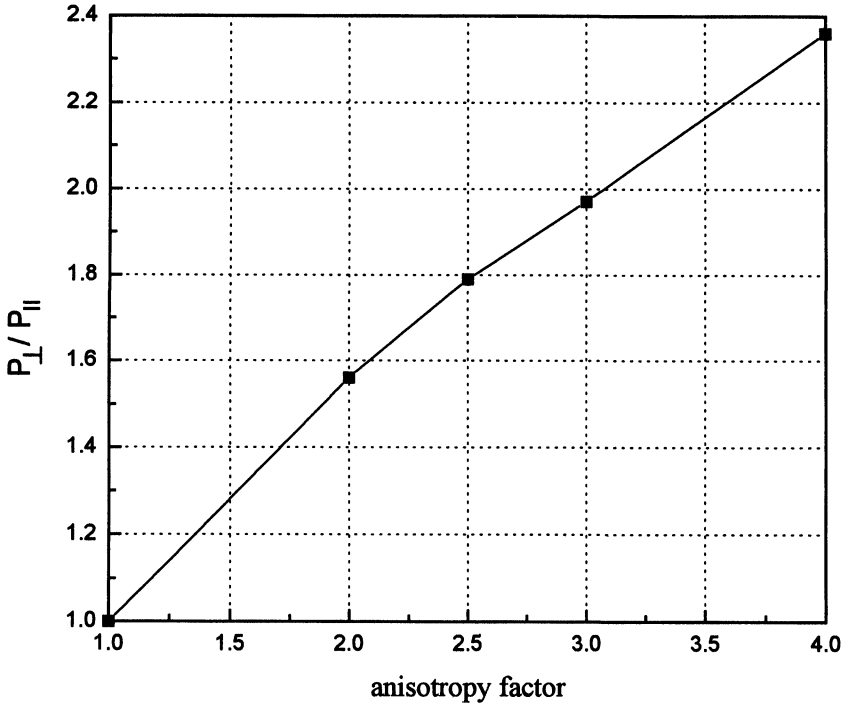

Figure 13 Calculated dependence of the grain ratio on the anisotropy factor with an aspect ratio > 3.5 ($P_{\perp}/P_{||}$) in sections perpendicular and parallel to the hot-pressing direction.

The calibration curve is shown in Figure 13.

The aspect ratio of three Si_3N_4-powders was measured. The theoretical anisotropy factor can be determined by means of the calibration curve with the calculated apparent aspect ratio [$P_{\perp}/P_{||}$] (Table 6).

A comparison between aspect ratio and texture is shown by this relationship. Quantitatively, the determined anisotropy factor has a much higher gradient than the calculated texture data. But, for an accurate description of the mathematical correlation, a larger number of values is necessary.

The differences can also be caused by the fact, that by X-ray diffraction all grains will be taken into account, whereas in the ceramographic method only the grains with a high aspect ratio (≥ 4) are considered.

Table 6 Comparison of calculated aspect ratio ($P_{\perp}/P_{||}$), the resulting anisotropy factor, the related texture index and the calculated (002) basal plane ratio.

Powder	*($P_{\perp}/P_{||}$) (AR ≥ 4)*	*Anisotropy Factor*	*Texture Index*	*I(00l)*
SNE 10	2.32	3.80	1.32	2.04
LC12SX	1.39	1.72	1.24	1.84
PP1	1.21	1.36	1.19	1.68

3.4.3 *Fracture Toughness*

It is expected, that the preferred orientation distribution of the nonrandom β-Si_3N_4 can be described by microstructural evidence. Toughness enhancements from crack-deflection (Liu *et al.*, 1989) and crack-bridging (Becker *et al.*, 1991) have intrinsic orientation dependences by intercrystal crack propagation (Figure 14).

This effect was demonstrated by fracture toughness measurements. The indentation was produced by the Vickers method parallel and perpendicular to the hot-pressing direction (Figure 2). The evaluation of the measured K_{Ic} calculated by the formula according to Anstis, is shown in Table 7.

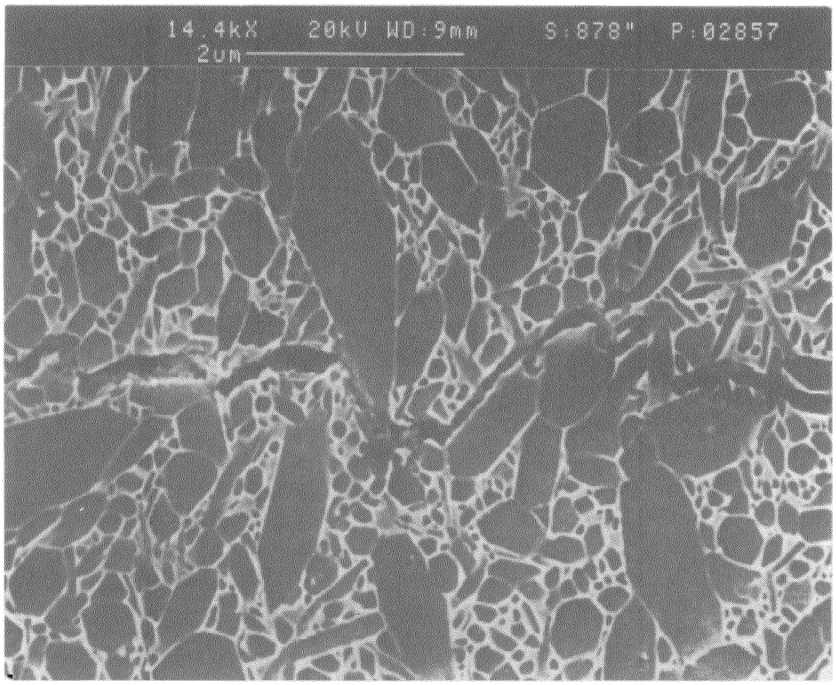

Figure 14 The intercrystal crack propagation in Si_3N_4-samples.

Table 7 Fracture toughness anisotropy.

Powder	*Indentation direction*	K_{Ic} $[MPa\sqrt{m}]$ 0°	↔	90°	ΔK_{Ic} $[MPa\sqrt{m}]$	*Texture Index*	ODF_{max}
SNE 10	⊥	5.3	↔	5.2	0.1	1.32	2.01
	∥	5.5	↔	3.9	1.6		
LC12SX	⊥	5.1	↔	5.0	0.1	1.24	1.89
	∥	5.2	↔	4.1	1.1		
PP1	⊥	4.4	↔	4.1	0.3	1.19	1.82
	∥	3.5	↔	2.8	0.7		

The K_{Ic}-values measured perpendicularly to the hot-pressing direction show only small differences. That confirms the measured rotational symmetry of the β-Si_3N_4 grains. In contrast, the crack lengths differences observed in parallel to the normal symmetry of the sample are considerable.

The result supports those from X-ray measured texture. The hot-pressed material has a preferred orientation of the long axes of the Si_3N_4-grains perpendicular to pressing direction. For a crack propagation parallel to the hot-pressing direction the crack-deflection is larger. This is attributed to the higher population of the grains at large angles between grains and the crack plane (Lee *et al.*, 1992). The result is a shorter crack length and a higher toughness. Perpendicular to the pressing direction, the toughness is lower because of the lower crack deflection. The toughness anisotropy is therefore determined by the degree of preferred orientation of β-Si_3N_4 grains.

A comparison of the ΔK_{Ic} values with the texture data shows, that the trend is significant. A stronger difference of the fracture toughness is attributed to higher texture anisotropy.

4. CONCLUSIONS

Summarizingly, the following statements can be made:

- Hot-pressed β-Si_3N_4 shows a ring-fibre texture with the basal plane (002) parallel to hot-pressing axis.
- The maximum intensity in this direction is about 2 times of random distribution.
- Powder properties of the starting powder like granulometric values, phase composition, and oxygen content influence the densification kinetics of Si_3N_4, the resulting volume fractions of α and β-phase and texture formation.
- The increase of the sintering aid ($Y_2O_3 + Al_2O_3$) favours the densification and leads to an acceleration of the process. The result is a weakness of the preferred anisotropy.
- The duration of isothermal time at 1800°C reinforces the texture strength of β-Si_3N_4 Long-time isothermal treatment enlarges the β-Si_3N_4 phase fraction. A reinforcement of the texture strength is the consequence of anisotropic growth.
- The delay of the load-application point during the phase transformation causes a slow down of the densification at low temperatures and reinforces the texture.
- A correlation between the fracture toughness anisotropy and the texture intensities can be proved.
- The aspect ratio of the β-Si_3N_4-grains confirmed the preferred orientation. A relationship with a model calculating the real aspect ratio can be shown.

The question of the texture mechanism between grain rotation and preferential grain growth cannot be answered completely. The densification curves (Figure 1) normally show two maxima of densification velocity. The maxima stand for the rearrangement- and dissolution-reprecipitation processes. In the case of a retarded load-application point the first maximum is as well retarded and leads to a higher densification before α-β transformation. The result is a texture reinforcement. This leads to the conclusion that the texture formation is a mechanical process of the existent needlelike grains over macroscopic flow processes as a reaction of the loaded pressure. On the other hand

the reinforcement of the texture during the isothermal time leads to the assumption that the preferential grain growth mechanism plays an important role in texture development. Probably both mechanisms participate in texture formation.

Acknowledgements

The authors thank D. Schläfer for assistance in the practical stages of this work. Support of the Deutsche Forschungsgesellschaft is gratefully acknowledged (Contract Nr. Ma 1531/1–1). Prof. Bunge is thanked for the valuable discussion and supply of the program 'HEXODF'.

References

Aldinger F. and Böcker W. D. G. (1992). *Entwicklung keramischer Hochleistungswerkstoffe*. Keramische Zeitschrift, **44**, Vol. 3, pp. 164–72.

Becker P. F. (1991). *Microstructural Design of Toughened Ceramics*. Journal of the American Ceramic Society, **74**, Vol. 2, pp. 255–69.

Bunge H. J. (1969). *Mathematische Methoden der Texturanalyse*. Akademie Verlag Berlin.

Bunge H. J. (1987). *Three-dimensional Texture Analysis*. International Material Reviews Vol. 32, pp. 265–290.

Herrmann M., Obenaus P., Schubert C., Stephan D. and Keßler S. (1992). *Characterization of the microstructure of anisotropic Si_3N_4-materials*. Metallography-conference Dresden.

Keßler S., Stephan D., Pabst J. and Schubert Chr. (1991). *Korntextur in heißgepreßtem Siliciumnitrid*. DGM Jahrestagung.

Keßler S. (1993). *Kristallisationsprozesse in heißgepreßter Siliciumnitridkeramik*. Dissertation Stuttgart.

Lee F. and Bowman K. J. (1992). *Texture and Anisotropy in Silicon Nitride*. Journal of the American Ceramic Society, **75**, Vol. 7, pp. 1784–1755.

Liu H., Weisskopf K. L. and Petzow G. (1989). *Crack Deflection Process for Hot-Pressed Whisker Reinforced Ceramic Composites*. Journal of the American Ceramic Society **72**, Vol. 4, pp. 559–563.

Mattern N., Riedel A. and Wassermann A. (1993). *Quantitative Phase Analysis of Si_3N_4 Ceramics using the Powder Diffraction Standard Data Base*. Material Scrience Forum, Vol. 133–136, pp. 39–44.

Munz D. and Fett T. (1989). *Mechanisches Verhalten keramischer Werkstoffe*. Springer-Verlag Berlin.

Pabst J., Boden G., Gerlach U., Herrmann M. and Schubert Chr. (1993). *Powder Properties Influencing the Densification Kinetics of Hot-Pressed Si_3N_4*. Material Sci. Forum, **70**, pp. 29–33.

Schubert Chr., Pabst J., Hermel W. and Klein U. (1989). *Computer-aided evaluation of the silicon nitride hot pressing compaction process*. DKG, **66**, Vol. 10, pp. 420–424.

Wassermann G. and Grewen J. (1962). *Texturen metallischer Werkstoffe*. Springer-Verlag Berlin.